Organosilicas with Chiral Bridges and Self-Generating Mesoporosity

Andreas Ide,[†] Rebecca Voss,[†] Gudrun Scholz,[‡] Geoffrey A. Ozin,[§] Markus Antonietti,[†] and Arne Thomas*,[†]

Department of Colloid Chemistry, Max Planck Institute of Colloids and Interfaces, Research Campus Golm, D-14424 Potsdam, Germany, Institute of Chemistry, Humboldt University of Berlin, D-12489 Berlin, Germany, and Materials Chemistry Research Group, Department of Chemistry, University of Toronto, 80 St. George Street, Toronto, Ontario M5S 3H6, Canada

Received December 20, 2006. Revised Manuscript Received March 9, 2007

Amine-functionalized, chiral mesoporous organosilicas were prepared from a rationally designed precursor, which combines the functions of a network builder, a chiral latent functional group, and a porogen in one molecule. The precursors are formed by a convenient enantioselective hydroboration using (*S*)-monoisopinocampheylborane on an ethylene-bridged silica precursor. These precursors do self-organize when hydrolysis of their inorganic moiety takes place via an aggregation of their organic moiety into hydrophobic domains. After a condensation−ammonolysis sequence mesoporous organosilicas functionalized with chiral amine groups are obtained, with the complete chiral functionalities located at the pore wall surface and therefore accessible to chemical processes. The pore size of the resulting organosilicas can be fine-tuned using different organic moieties attached to the boron group in the first step. While a wormlike arrangement of pores is observed for the pure precursor, common surfactants can be admixed to further control and tailor the resulting mesoporous system. In certain phase ranges, also chiral *periodic* mesoporous organosilicas can be obtained.

Introduction

Porous bridged organosilicas, as represented by aerogels of polysilsesquioxanes[1] or the surfactant-mediated periodic mesoporous organosilicas (PMOs),[2,3] combine the unique features of porous glasses, such as high surface areas and defined pore structures, with the chemical functionality and physical properties of organic materials. By introduction of silica-bridging organic linkers into highly porous silica frameworks, materials with tunable functionality and new mechanical, electronic, and optical properties can be prepared, leading to potential applications in catalysis, sensing, microelectronics, and separation.[4−7] Compared to porous silicas with grafted organic groups, bridged organosilicas exhibit some important advantages, mainly the high organic loading possible under preservation of the mechanical stability while even smaller pores are only insignificantly blocked.

However, the homogeneous distribution of organic groups in the silica framework does not necessarily make them located at the pore wall and accessible for further modifications, which is a vital point for applications, e.g., in catalysis and chromatographic separation. In contrast, usually a significant fraction of the organic groups are nonaccessible, buried through condensation within the pore walls. Ozin et al. demonstrated that the organic groups in an ethylene-bridged organosilica could not be further functionalized with hydroborane, normally a highly reactive reagent, while terminal vinyl groups introduced in the same PMO where fully converted.[8] This proves that a control of the properties of the organosilica does not exclusively rely on the choice of the organic groups, but also on their position in the silica framework. To exploit the full potential of porous organosilicas, the organic groups should be positioned at the pore walls, making them accessible for reagents or substrates entering the pores.

Another requirement in the synthesis of functional organosilicas is that the organic groups, introduced into the bridged organosilica precursors, should not interfere with the subsequent sol−gel process. This excludes some viable organic functional groups, and while the functionalization of mesoporous silicas with grafted amines has been frequently described,[9] just a few examples of porous bridged organosilicas with directly incorporated functional groups such as amines are reported.[10−12] We recently described an

* To whom correspondence should be addressed. E-mail: Arne.Thomas@mpikg.mpg.de.
[†] Max Planck Institute of Colloids and Interfaces.
[‡] Humboldt University of Berlin.
[§] University of Toronto.

(1) Loy, D. A.; Jamison, G. M.; Baugher, B. M.; Russick, E. M.; Assink, R. A.; Prabakar, S.; Shea, K. J. *J. Non-Cryst. Solids* **1995**, *186*, 44.
(2) Asefa, T.; Yoshina-Ishii, C.; MacLachlan, M. J.; Ozin, G. A. *J. Mater. Chem.* **2000**, *10*, 1751.
(3) Yoshina-Ishii, C.; Asefa, T.; Coombs, N.; MacLachlan, M. J.; Ozin, G. A. *Chem. Commun.* **1999**, 2539.
(4) Chevalier, P.; Corriu, R. J. P.; Delord, P.; Moreau, J. J. E.; Man, M. W. C. *New J. Chem.* **1998**, *22*, 423.
(5) Hatton, B.; Landskron, K.; Whitnall, W.; Perovic, D.; Ozin, G. A. *Acc. Chem. Res.* **2005**, *38*, 305.
(6) Hoffmann, F.; Cornelius, M.; Morell, J.; Froba, M. *J. Nanosci. Nanotechnol.* **2006**, *6*, 265.
(7) Shea, K. J.; Loy, D. A. *Chem. Mater.* **2001**, *13*, 3306.
(8) Asefa, T.; Kruk, M.; MacLachlan, M. J.; Coombs, N.; Grondey, H.; Jaroniec, M.; Ozin, G. A. *J. Am. Chem. Soc.* **2001**, *123*, 8520.
(9) Chong, A. S. M.; Zhao, X. S. *J. Phys. Chem. B* **2003**, *107*, 12650.
(10) Corriu, R. J. P.; Mehdi, A.; Reye, C.; Thieuleux, C. *Chem. Commun.* **2002**, 1382.

10.1021/cm063026j CCC: $37.00
Published on Web 04/20/2007

"all-in-one" approach to control the placement of organic functionalities exclusively along pore interfaces.[13] This was achieved by a hydroboration reaction on an ethylene-bridged silica precursor and the subsequent fixation of a sterically demanding group to this functional monomer. During condensation this precursor self-organized comparable to amphiphilic molecules, with the organic moieties aggregated in hydrophobic domains. Subsequent ammonolysis yielded a mesoporous organosilica with amine groups placed exclusively at the pore surfaces. This approach differed significantly from other strategies, where the organic group of the precursor was used as a template for porosity: There, the organic bridging group is removed, e.g., via calcination, creating a porosity,[14−17] which is however accompanied by a structural weakening of the organosilica framework. In contrast, in our approach just appending parts of the organic moieties were selectively cleaved, maintaining the bridging organic group, while introducing a viable functionality on the pore wall only.

Besides functionality, the introduction of chirality into bridged organosilicas is of special interest. Several groups reported on the introduction of chiral organic groups into mesoporous bridged organosilicas.[18−23] It was shown that these chiral mesoporous organosilicas (ChiMOs) display optical activity and even exhibit enantioselective discrimination. Therefore, these materials are highly promising candidates in applications such as chromatography of optical isomers or enantioselective catalysis. However, in most approaches the chiral organic groups were attached to the silane groups via long and flexible linkers. Even though bridge bonded, these organic groups can therefore hardly be regarded as a supporting component of the pore walls, and consequently, the addition of high amounts of pure inorganic precursors was necessary to stabilize the porous framework. Recently, Polarz et al. synthesized a chiral PMO precursor related to the above-mentioned "all-in-one" approach.[24] An ethylene-bridged precursor was converted into a chiral alcohol using a metal-catalyzed, enantioselective hydroboration with subsequent oxidative alcoholysis. Hydrolysis and condensation of this precursor in the presence of surfactants yielded PMOs with ordered pore systems, while the preservation and accessibility of the chiral functions in the resulting silica were not further proven.

Herein we report on the rational design of a new chiral organosilica precursor. This precursor is convertible into an amine-functionalized, chiral mesoporous organosilica via a condensation−ammonolysis sequence. The so-prepared organosilicas exhibit a tunable functionality and porosity and a very high and accessible surface area. The chirality in our case is brought on by an enantioselective hydroboration using (*S*)-monoisopinocampheylborane. This approach has several advantages: Compared to metal-catalyzed reactions, higher enantioselectivities were reported ((*E*)-alkenes are converted with up to 95% ee).[25] Furthermore, the as-made monomers do self-organize when hydrolysis of their inorganic part takes place, yielding an aggregation of the organic parts into hydrophobic domains and subsequently, after their removal, porous materials with the activated amine sites accessible at the pore interface. The size of the hydrophobic domains can be tailored by attaching sterically demanding alkenes or alcohols to the monomers, resulting in different pore sizes. Stereoselective splitting of the carbon−boron bonds after condensation of the organosilica network yields a chiral functional group localized at the pore wall by the template moiety. Even though the precursors are self-organizing, also common surfactants can be admixed to further control and tailor the resulting mesoporous system and finally create also chiral *periodic* mesoporous organosilicas.

Experimental Section

Materials. Bis(triethoxysilyl)ethene was synthesized by alkene metathesis of (triethoxysilyl)ethene.[26] (Triethoxysilyl)ethene was purchased from Gelest. Boron trifluoride diethyl etherate, hydroxylamine-*O*-sulfonic acid, tetraethoxysilane (TEOS), and (*S*)-Alpine-Boramine were obtained from Aldrich. Solvents for reactions under moisture exclusion were prepared according to standard procedures. All further commercial chemicals were used without additional purification.

Preparation of the Boron-Containing Precursor. The reaction was carried out under a N_2 atmosphere. In a typical synthesis 4.80 g (11.7 mmol) of the (*S*)-Alpine-Boramine was dissolved in 40 mL of dry THF at 0 °C, and then 2.90 mL (23.3 mmol) of boron trifluoride diethyl etherate was added. After 20 min the reaction mixture was warmed to room temperature (rt) and stirred for another 4 h. The precipitate was filtered off and washed with dry THF. The clear solution was cooled to −20 °C, and 8.06 g (22.9 mmol) of bis(triethoxysilyl)ethene was slowly added. While being stirred for 18 h, the mixture was allowed to warm to rt. According to the desired product, the appropriate alcohol (22.9 mmol) was added at 0 °C, and the solution was stirred for another 2 h. The solvent was removed under vacuum. Addition of heptane led to precipitation of a white solid, which was centrifuged off. The solid was washed with heptane, and the solvent was removed to give the corresponding chiral precursor. ^{1}H NMR (CBS, 400 MHz): δ 0.95 (br m, 18 H, aliphatic H), 1.17 (t, J = 6.8 Hz, 9 H, $SiOCH_2CH_3$), 1.18 (t, J = 6.8 Hz, 9 H, $SiOCH_2CH_3$), 1.41 (m br, 5 H, aliphatic H), 3.79 (q, J = 6.8 Hz, 6 H, $SiOCH_2$), 3.80 (q, J = 6.8 Hz, 6 H, $SiOCH_2$), 3.84 (q, J = 6.8 Hz, 2 H, $BOCH_2$). ^{1}H NMR (CBS-C16, 400

(11) Wahab, M. A.; Imae, I.; Kawakami, Y.; Ha, C. S. *Chem. Mater.* **2005**, *17*, 2165.
(12) Wahab, M. A.; Kim, I.; Ha, C. S. *J. Solid State Chem.* **2004**, *177*, 3439.
(13) Voss, R.; Thomas, A.; Antonietti, M.; Ozin, G. A. *J. Mater. Chem.* **2005**, *15*, 4010.
(14) Boury, B.; Chevalier, P.; Corriu, R. J. P.; Delord, P.; Moreau, J. J. E.; Chiman, M. W. *Chem. Mater.* **1999**, *11*, 281.
(15) Shea, K. J.; Loy, D. A.; Webster, O. *J. Am. Chem. Soc.* **1992**, *114*, 6700.
(16) Boury, B.; Corriu, R. J. P.; Le Strat, V. *Chem. Mater.* **1999**, *11*, 2796.
(17) Boury, B.; Corriu, R. J. P. *Adv. Mater.* **2000**, *12*, 989.
(18) Benitez, M.; Bringmann, G.; Dreyer, M.; Garcia, H.; Ihmels, H.; Waidelich, M.; Wissel, K. *J. Org. Chem.* **2005**, *70*, 2315.
(19) Alvaro, M.; Benitez, M.; Das, D.; Ferrer, B.; Garcia, H. *Chem. Mater.* **2004**, *16*, 2222.
(20) Baleizao, C.; Gigante, B.; Das, D.; Alvaro, M.; Garcia, H.; Corma, A. *Chem. Commun.* **2003**, 1860.
(21) Jiang, D. M.; Yang, Q. H.; Wang, H.; Zhu, G. R.; Yang, J.; Li, C. *J. Catal.* **2006**, *239*, 65.
(22) Brethon, A.; Hesemann, P.; Rejaud, L.; Moreau, J. J. E.; Man, M. W. C. *J. Organomet. Chem.* **2001**, *627*, 239.
(23) Moreau, J. J. E.; Vellutini, L.; Man, M. W. C.; Bied, C. *J. Am. Chem. Soc.* **2001**, *123*, 1509.
(24) Polarz, S.; Kuschel, A. *Adv. Mater.* **2006**, *18*, 1206.
(25) Brown, H. C.; Ramachandran, P. V. *J. Organomet. Chem.* **1995**, *500*, 1.
(26) Marciniec, B.; Maciejewski, H.; Gulinski, J.; Rzejak, L. *J. Organomet. Chem.* **1989**, *362*, 273.

Scheme 1. Synthesis of Chiral MO Precursors via Hydroboration with (*S*)-Isopinocampheylmonoborane and Hydrolysis, Condensation, and Ammonolysis of the Precursor

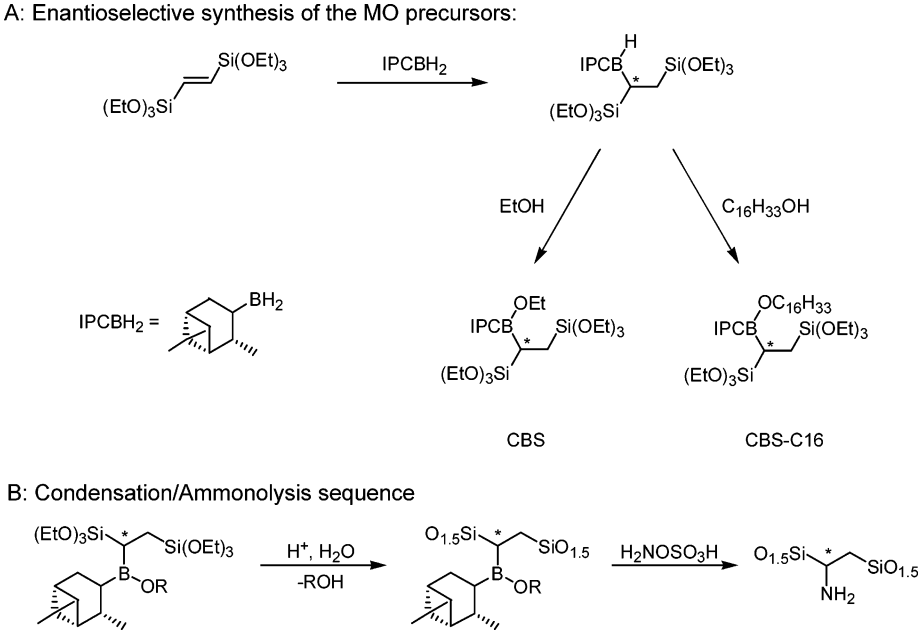

MHz): δ 0.87 (m, 7 H, aliphatic H), 1.06 (m, 4 H, aliphatic H), 1.16 (m, 16 H, aliphatic H), 1.20 (m, 21 H, aliphatic H), 1.23 (m, 18 H, $SiOCH_2CH_3$), 1.51 (m, 3 H, aliphatic H), 3.80 (m, 14 H, $BOCH_2$, $SiOCH_2$).

Condensation of the Boron-Containing Precursor. Various silicas were synthesized by modifying the precursor/TEOS ratios (see Table 1). Regardless of the ratio precursor/TEOS, all reaction mixtures contained a total amount of 5.00 mmol of silicon. These mixtures were dissolved in 3.0 mL of ethanol, and then 0.6 mL of hydrochloric acid (pH 2.0) was added. The solution was homogenized in a closed vial for 5 min at rt. The silica solution was then aged for 2 days at 60 °C to give the monolithic solids.

Functionalization. The crude silica condensate was mechanically crushed, and 0.35 g of the crude powder was dispersed in 5.0 mL of diglyme. For every 1 mmol of boron contained in the silica, 2 mmol of hydroxylamine-*O*-sulfonic acid was added. The mixture was stirred at 60 °C for 3 h. After the suspension was cooled to rt, the solvent was removed by centrifugation. To completely remove the excess hydroxylamine-*O*-sulfonic acid and the cleaved organic residue, the resulting material was stirred in 20 mL of HCl (pH 2) for 4 h and then repeatedly washed with water, ethanol, and THF. All solvents were removed under vacuum at 60 °C to give a white solid.

PMO Synthesis (CBS-F127). For the synthesis of a chiral periodic mesoporous organosilica, 0.5 g of Pluronic F-127 was dissolved in 10.0 mL of absolute ethanol, and then 0.10 g (0.19 mmol) of chiral precursor, 0.16 g (0.76 mmol) of TEOS, and 50 μL of HCl (pH 2) were added. The mixture was stirred for 20 min at rt. The clear solution was added to a Petri dish and aged at rt for 5 h and then additionally at 80 °C for 23 h. The pale solid was mechanically crushed, dispersed in 20 mL of ethanol, and stirred overnight at 60 °C to extract the surfactant. Functionalization by ammonolysis was carried out analogously to that of the CBS samples prepared without surfactants. Further purification was carried out by repeated washing/centrifugation with 20 mL of ethanol and 20 mL of acetone. After the sample was dried under vacuum for 2 h at 60 °C a white solid was obtained.

Characterization of the Precursor and Porous Materials. Transmisson electron microscopy (TEM) images were taken using a Zeiss EM 912Ω operated at an acceleration voltage of 120 kV. Samples were ground in a ball mill and dispersed in acetone. One droplet of the suspension was applied to a 400 mesh carbon-coated cooper grid and left to dry in the air.

Nitrogen adsorption data were obtained with a Quantachrome Autosorb-1 at liquid nitrogen temperature.

SAXS measurements were done using a Bruker saxs D8-advance.

FTIR spectra were collected using a BIORAD FTS 6000 spectrometer equipped with an attenuated total reflection (ATR) setup.

^{29}Si, ^{11}B, and $^{1}H \rightarrow {}^{13}C$ CP MAS NMR spectra were recorded on a Bruker AVANCE 400 spectrometer (Larmor frequencies: ν_{29Si} = 79.5 MHz; ν_{11B} = 128.4 MHz, ν_{1H} = 400.1 MHz, ν_{13C} =100.6 MHz) using a 4 mm MAS probe (Bruker Biospin) and applying a spinning speed of 10 kHz. ^{29}Si MAS NMR (I = 1/2) spectra with 2750 accumulations were recorded with a $\pi/2$ pulse duration of p1 = 4.25 μs, a spectrum width of 20 kHz, and a recycle delay of 120 s. ^{11}B MAS NMR (I = 3/2) spectra were recorded with an excitation pulse duration of 1 μs and referenced with respect to the chemical shift of ^{11}B in $BF_3{\cdot}OEt_2$. The recycle delay was chosen as 1 s, and the accumulation number was 1800. The contact times of the $^{1}H \rightarrow {}^{13}C$ CP MAS NMR experiments were optimized as 1 ms for the boron-containing precursor and 0.25 ms after ammonolysis. Values of the isotropic chemical shifts of ^{1}H, ^{13}C, and ^{29}Si are given with respect to the peak for TMS.

^{1}H NMR spectra were recorded on a Bruker DPX 400 spectrometer in $CDCl_3$ solution. For the calibration $CDCl_3$ signals (δ = 7.24 ppm) were used.

For the circular dichroism measurements a J-715 spectrometer from Jasco was used. All samples were dispersed in $CHCl_3$ and measured in a 1 mm quartz cuvette (data pitch 0.2 nm, bandwidth 2.0 nm, response 2 s). For each spectrum five single measurements were accumulated and corrected by subtraction of the baseline.

Results and Discussion

Porous chiral amine-functionalized organosilicas were synthesized via enantioselective hydroboration of an ethylene-bridged organosilica precursor, condensation of this precursor, and finally ammonolysis of the boron moieties

Table 1. Organosilicas Prepared in This Study

entry	Si_{CBS}/Si_{TEOS} ratio	precursor/ amt (mmol)	TEOS amt (mmol)	HCl vol (mL)	EtOH vol (mL)
CBS-1	1/0	CBS/2.50		0.6	3.0
CBS-2	1/2	CBS/1.25	2.50	0.6	3.0
CBS-3	1/4	CBS/0.83	3.33	0.6	3.0
CBS-4	1/8	CBS/0.50	4.00	0.6	3.0
CBS-C16-1	1/0	CBS-C16/2.50		0.6	3.0
CBS-C16-2	1/2	CBS-C16/1.25	2.50	0.6	3.0
CBS-C16-3	1/4	CBS-C16/0.83	3.33	0.6	3.0

(Scheme 1). As an enantioselective hydroboration reagent, commercially available (*S*)-monoisopinocampheylborane was used. Either the reaction was quenched with ethanol, yielding a compound denoted as CBS, or the intermediate was further reacted with hexadecanol (denoted as CBS-C16), causing an increase of the hydrophobic domain to promote the self-organization of the precursor. We observed that the remaining borane site could also be reacted with terminal alkenes. Precursors synthesized using 1-hexadecene however yield results comparable to those for precursors reacted with hexadecanol; thus, just data of the alcohol-quenched precursors are described in the following.

The reaction can be monitored using ^{1}H NMR measurements (Figure S1 in the Supporting Information (SI)). It is seen that the ethylene protons of the starting material have vanished completely in the spectra of the products, proving the full conversion by addition of the borane. Additional signals corresponding to alkane protons can be attributed to the campheyl and bridging ethane groups, respectively. The hydroboration reaction was further verified by FT-IR measurements (Figure S2 in the SI). The appearance of C−H, C−B, and O−B deformation modes between 1250 and 1460 cm^{-1} supports the successful hydroboration. Additional peaks arising at 858 and 888 cm^{-1} can be assigned to CH vibrations of branched chain alkanes. The observed increased intensity of the CH stretching modes between 2880 and 2980 cm^{-1} is due to the addition of the campheyl moiety. As expected, no signals above 3000 cm^{-1} are observed for CBS precursors, which would be indicative of C═C−H vibrational modes. However, a comparative IR measurement of bis(triethoxysilyl)ethane and bis(triethoxysilyl)ethene revealed that CH double bond vibrational modes are unobservably weak for these precursors and therefore not suitable for monitoring the here-described hydroboration.

The precursors display optical activity confirmed by circular dichroism measurements.

Organosilicas were synthesized from this precursor using a bulk condensation procedure with hydrochloric acid for condensation of the bridged silica moieties. In Table 1, the synthetic details of the organosilicas under discussion are summarized.

In the first series, a set of silicas was produced from the CBS precursor and different amounts of TEOS and HCl (pH 2). Stereoselective splitting of the carbon−boron bonds after condensation of the organosilica network was carried out by stirring of the materials in hydroxylamine-*O*-sulfonic acid/diglyme solutions. This procedure leads to functionalization on the organic bridges. Extraction of the cleaved organic attachments is mainly accomplished during this functionalization step, while the complete removal of the organic moieties can be obtained after an additional extraction with ethanol and THF (see Figure S3 in the SI). It should be noted that this approach can naturally also lead to other functional groups attached to the bridges, as various transformations toward versatile functionalities are known from chiral organoboranes.[25]

The condensation and functionalization step was analyzed using ^{29}Si, ^{11}B (Figure 1), and ^{13}C (Figure S4 in the SI) MAS NMR and IR measurements (Figure S3 in the SI). For the condensed but not functionalized material ^{29}Si NMR resonances appear between −60 and −85 ppm representative of T-type organosilica species, while the weak signal for Q units at −110 ppm confirms that Si−C bond cleavage is only minor. Deconvolution of the spectra arrived at an integral proportion of about 10% for the Q sites. The same is true for materials after ammonolysis, proving that the bridge-bonded organic group is maintained throughout the reaction. Changes in the coordination of the bridge-bonded organic group after ammonolysis have a distinct influence on the ^{29}Si signals. The spectrum in Figure 1b can be simulated with at least three different T species at −83, −75, and −65 ppm, respectively. These signals can be attributed to T^1, T^2, and T^3 species; however, a reliable assignment is difficult because these T sites are also likely to be observed due to the (rarely described) asymmetric composition of the organosilica, where the silica atoms are bound to two different carbon species of the bridging group. This asymmetric bridging group should therefore result in the emergence of, e.g., two T_3 species. The strong signal at −75 ppm after ammonolysis, exhibiting a 1/1 ratio to the strong signal at −83 ppm, therefore can be attributed to the formation of a new T_3 species as expected for this reaction.

A comparison of the ^{11}B NMR spectra for both materials shows a strong signal for the as-made organosilica, which has significantly weakened after ammonolysis (Figure 1c). However, the appearance of this, even though weak, signal indicates that a few boron moieties are trapped in the silica framework, thus not accessible for further functionalization. A comparison of the spectra in Figure 1c indicates the existence of at least two boron species before functionalization, and only one, the accessible one, disappears after ammonolysis. Comparable results are observed from the ^{13}C NMR spectra where the signals attributable to the boron-attached campheyl and ethanol groups have weakened significantly (Figure S4), showing the almost complete cleavage of the boron moieties.

Additional IR measurements on the condensed materials before and after functionalization support these results. The CH_3, CH_2, and CH stretching vibrations at 2900 cm^{-1} nearly disappeared in the functionalized samples, proving the successful cleavage and removal of the campheyl and hexadecyl moieties. The same is true for the CH_3, CH_2, CH, B−C, and B−O deformation vibrations, which can be assigned to the broad band at 1365 cm^{-1}. As functionalization yields almost complete removal of the hydrocarbons, the remaining CH groups causing only very weak signals. Due to the high amine loading, especially for sample CBS-1, a new peak at 1632 cm^{-1} can be identified after functionalization, which can be assigned to NH_2 deformation modes.

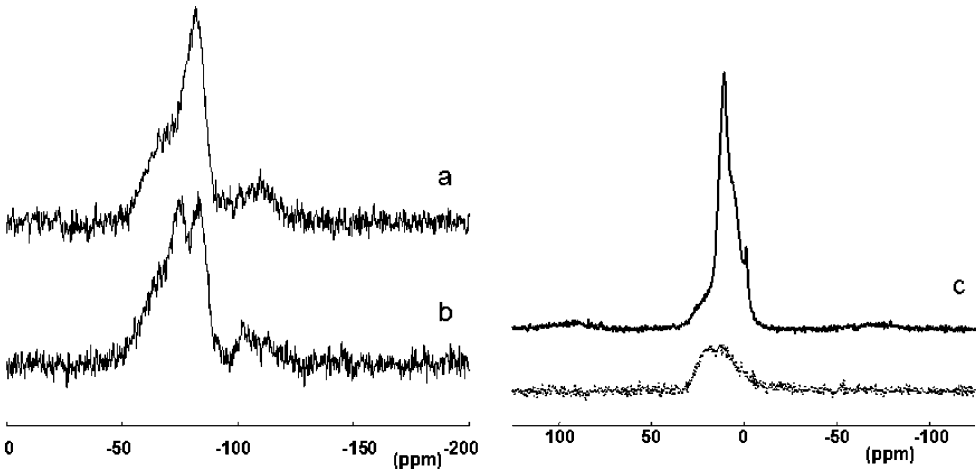

Figure 1. ^{29}Si and ^{11}B MAS NMR spectra before and after ammonolysis of organosilica CBS-1: (a) ^{29}Si before ammonolysis, (b) ^{29}Si after ammonolysis, (c) ^{11}B before and after (dotted line) ammonolysis.

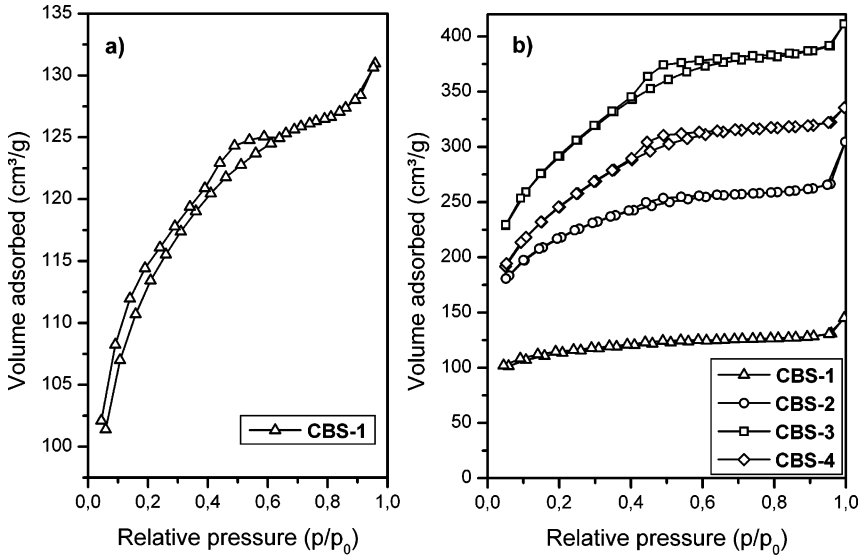

Figure 2. (a) N_2 sorption isotherms of sample CBS-1 and (b) comparison of samples CBS-1−4 showing the influence of different CBS/TEOS ratios on the observed porosity and surface area.

However, the typically existing NH stretching modes at 3100 cm^{-1} are presumably buried under the broad vibration band of adsorbed water and therefore not suitable for characterization.

It is important to note that the removal of the organic moiety is not accompanied by a significant bridge cleavage. This shows that the part of the organosilica responsible for the network formation is preserved intact after the functionalization by ammonolysis and the extraction step. It therefore can be assumed that the resulting organosilica framework is also stable enough to maintain porosity after removal of the organic moieties.

The resulting materials were analyzed using nitrogen sorption, TEM, and XRD measurements. All organosilicas showed no detectable porosity and surface area prior to ammonolysis. However, after this functionalization, defined porosities and high surface areas are observed. The BET isotherms of the materials CBS-1−4 after ammonolysis are shown in Figure 2.

The isotherms for organosilicas made from the pure precursor (CBS-1) exhibit a high nitrogen uptake at low relative pressures and a less pronounced hysteresis, indicating the existence of mainly micropores (<2.0 nm) and some additional mesopores (>2.0 nm) in this sample (Figure 2a). Furthermore, the surface area is considerably lowered compared to that of the materials with admixed TEOS. It is also observed that the adsorption and desorption branches do not close at low relative pressure, indicating a soft, polymer-like material. This probably yields a partial collapse of the porous system for the pure organosilica (CBS-1) after functionalization and extraction of the organic moiety.

All other organosilicas exhibit high surface areas of up to 1000 m^2/g for CBS-3 and average pore sizes in the range of 2.2−2.6 nm, which is significantly higher than found for molecular imprinting of related organic molecules (0.8 nm).[27] Regarding our prior work on boron-functionalized organosilicas as supporting evidence, an aggregation of the hydrophobic moieties of the monomer can be assumed, yielding an increased pore size compared to that of silicas generated by single-molecule templating (Scheme 2).

(27) Hunnius, M.; Rufinska, A.; Maier, W. F. *Microporous Mesoporous Mater.* **1999**, *29*, 389.

Table 2. BET Surface Area and Pore Size Characterization for Organosilicas CBS-1−4 after Ammonolysis

sample	a_S(BET)[a] (m^2/g)	d_P(NLDFT)[b] (nm)	$V_{p,micro}$(NLDFT)[c] (cm^3/g)	$V_{p,meso}$(NLDFT)[d] (cm^3/g)	$V_{p,tot}$(NLDFT)[e] (cm^3/g)
CBS-1	367	2.0	0.143	0.041	0.184
CBS-2	731	2.2	0.186	0.166	0.352
CBS-3	1010	2.6	0.165	0.379	0.544
CBS-4	853	2.5	0.141	0.316	0.457

[a] Specific BET surface area. [b] Average pore diameter. [c] Micropore volume of pores >2 nm in diameter. [d] Mesopore volume of pores between 2 and 50 nm in diameter. [e] Total pore volume (sum of micro- and mesopore volumes).

Scheme 2. Self-Assembly of CBS Precursors and the Porosity Generated after Ammonolysis

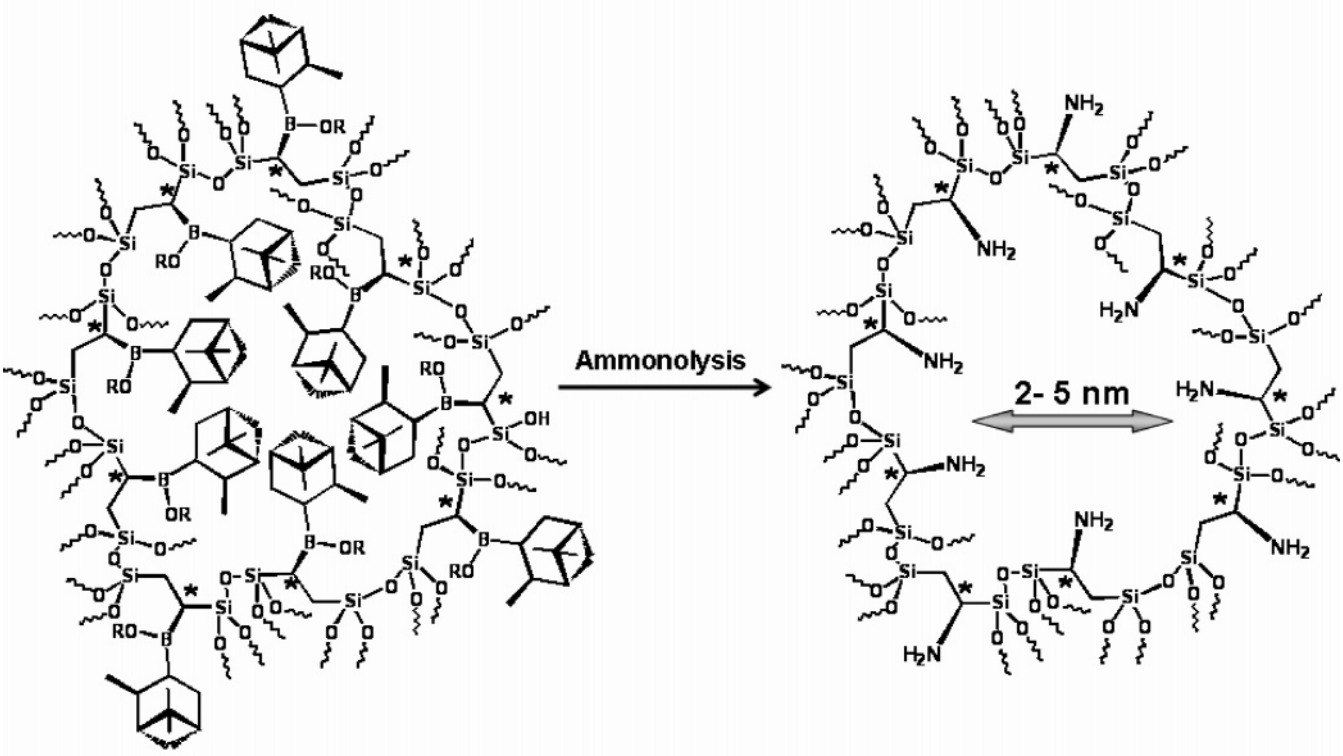

Table 2 compares the BET surface areas, the average pore diameters from DFT evaluation, and the micro- and mesopore volumes of samples CBS-1−4. Distinctly higher surface areas and increasing average pore diameters are observed for materials prepared with addition of pure silica precursor, more precisely for intermediate TEOS/CBS ratios. This can be attributed to a stabilization of the organosilica framework with increasing amount of the stiff inorganic parts. To avoid pore collapsing, reinforcement of organosilica frameworks by addition of pure silica precursors is frequently used throughout the literature, especially for chiral mesoporous organosilicas (however with much higher TEOS/ChiMO precursor ratios).[19,20] Note that for long and flexible bridging groups, a significant amount of TEOS has to be added, e.g., for the generation of PMOs, yielding an overall decrease of the organic groups in the framework.

Therefore, it is interesting to note that also for the pure organosilica (CBS-1 made without addition of the purely inorganic comonomer) a still significant surface area is observed. This proves that the chiral-bridged organosilica is mechanically strong enough to at least partially support the pore wall, allowing an organic monomer content of 100%.

The comparison of micro/mesopore volumes for CBS-1−4 furthermore indicates that, besides the stabilization of the pore walls, the addition of pure silica precursor enhances the aggregation of the organic moieties, as a higher fraction of mesopores is observed in the samples with a higher pure inorganic precursor content.

Thus, from the BET measurements it is seen that for a TEOS/CBS molar ratio of 4/1 the maximal porosity is observed. Further addition of TEOS then again leads to a decrease of the surface area, which can be expected due to the increasing silica content, which does not contribute to the overall porosity. The ratio of the micro- and mesopore volumes (Table 2) of samples CBS-3 and -4 are comparable to those of other mesoporous silicas exhibiting smaller mesopores, e.g., derived from Brij surfactants.[28] However, due to the less defined aggregation of the hydrophobic moieties, the CBS materials possess a much less defined pore size distribution.

The pore architectures and especially the pore size of the resulting mesoporous organosilica can be further modified when long-chain alkyl tails are additionally attached to the precursor (CBS-C16). In Figure 3 the BET isotherms of pure and TEOS-admixed organosilicas prepared from CBS-C16 are shown. The pure precursor (CBS-C16) exhibits already a considerable surface area; however, an average pore size

(28) Thomas, A.; Polarz, S.; Antonietti, M. *J. Phys. Chem. B* **2003**, *107*, 5081.

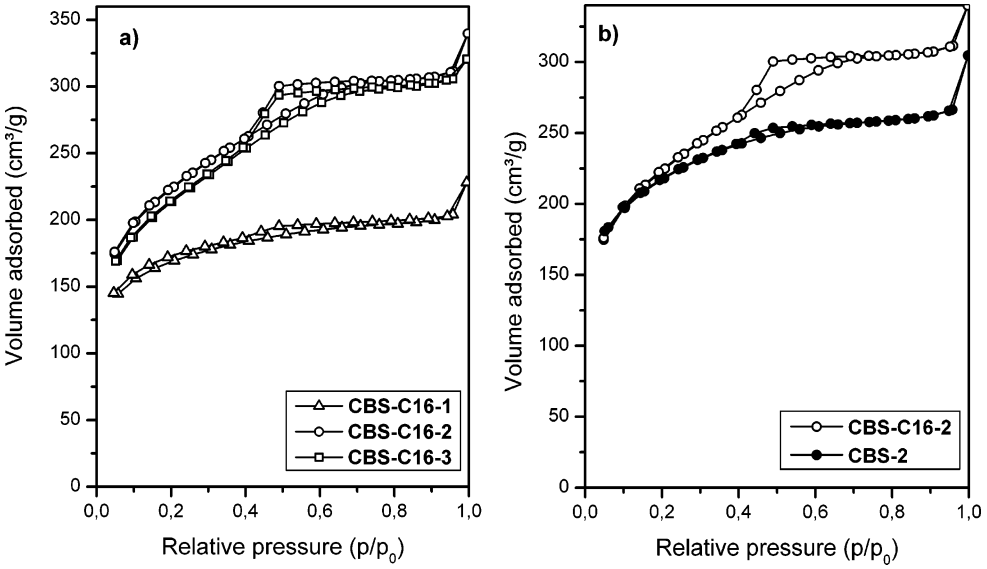

Figure 3. (a) N_2 sorption isotherms of samples CBS-C16-1−3 and (b) comparison of N_2 sorption isotherms for organosilicas CBS-2 and CBS-C16-2.

Table 3. BET Surface Area and Pore Size Characterization for Organosilicas CBS-C16-1−3 after Ammonolysis

sample	a_S(BET)[a] (m^2/g)	d_P(NLDFT)[b] (nm)	$V_{p,micro}$(NLDFT)[c] (cm^3/g)	$V_{p,meso}$(NLDFT)[d] (cm^3/g)	$V_{p,tot}$(NLDFT)[e] (cm^3/g)
CBS-C16-1	559	2.0	0.167	0.117	0.284
CBS-C16-2	771	5.1	0.129	0.288	0.417
CBS-C16-3	739	4.6	0.116	0.296	0.412

[a] Specific BET surface area. [b] Average pore diameter. [c] Micropore volume of pores <2 nm in diameter. [d] Mesopore volume of pores between 2 and 50 nm in diameter. [e] Total pore volume (sum of micro- and mesopore volumes).

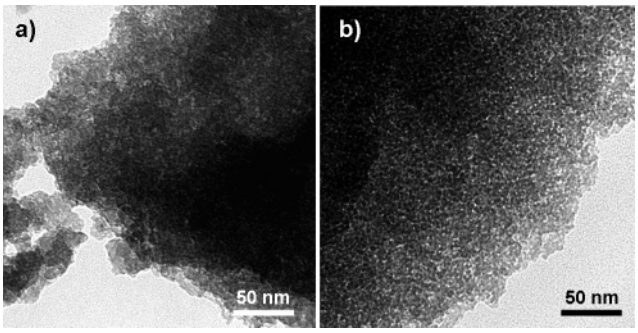

Figure 4. TEM measurements on the silicas (a) CBS-2 and (b) CBS-16-2 after ammonolysis and extraction.

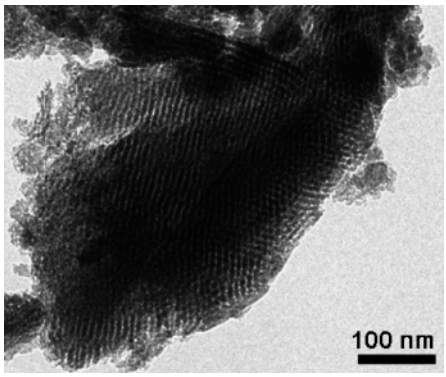

Figure 5. TEM micrograph of CBS-F127 after extraction of the surfactant and ammonolysis.

not higher than that for the CBS precursors is observed. Comparable to the organosilica CBS-1, this is due to a partial collapse of the porosity, as a result of the high organic fraction in this sample. This is supported by the finding that the highest surface area as well as a more defined mesoporosity is observed for the organosilicas prepared by admixing TEOS. As summarized in Table 3, the pore sizes for these organosilicas have increased up to 5 nm, showing the influence of the attached hexadecyl chains by increasing the hydrophobic domains and the related pore size. The comparison of organosilicas made from CBS and CBS-C16 under otherwise similar conditions nicely illustrates this finding (Figure 3b), as a more pronounced hysteresis, indicative of larger fractions of mesopores, is observed for the CBS-C16.

TEM measurements (Figure 4) on the materials indicate the presence of a disordered, wormlike pore structure. Even though the campheyl attachments are able to form hydrophobic aggregates and subsequently lyotropic phases, these phases are not long range ordered.

This yields materials with high surface areas and mesoporosity, but without regularity of the pores. This finding, however, is certainly no disadvantage for most applications, because disordered systems suffice the needs of membrane technology or catalysis, which do not directly benefit from mesoscopic order.[29] Nevertheless, to prove the versatility of this precursor, we also tried to use it in a conventional PMO synthesis, using a common triblock copolymer (Pluronic F127) as the template. Pluronic-type triblock copolymers have been frequently used for the preparation of PMOs.[30−32] As shown in Figure 5 organosilicas with an ordered pore structure are formed—proving that the present concept and monomer system can also be expanded to *periodic* meso-

(29) Rolison, D. R. *Science* **2003**, *299*, 1698.
(30) Muth, O.; Schellbach, C.; Froba, M. *Chem. Commun.* **2001**, 2032.
(31) Hunks, W. J.; Ozin G. A. *Adv. Funct. Mater.* **2005**, *15*, 259.
(32) Guo, W. P.; Li, X.; Zhao, X. S. *Microporous Mesoporous Mater.* **2006**, *93*, 285.

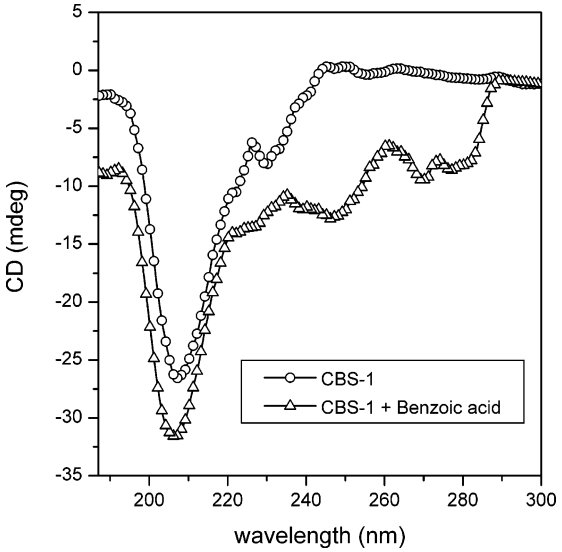

Figure 6. Circular dichroism measurements of the precursor CBS, organosilica CBS-1, and organosilica CBS-1 after addition of benzoic acid.

porous silicas. Nitrogen sorption measurements (Figure S5 in the SI) reveal a specific BET surface area of 591 m^2/g for this CBS-F127 PMO. NLDFT evaluation of the pore diameter using the adsorption branch (Figure S5) and SAXS measurements (Figure S6 in the SI) furthermore indicate a narrow pore size distribution with a maximum at 5.1 nm for the amine-functionalized material.

For evaluation of the chiral properties of the organosilicas, circular dichroism measurements were carried out on the condensed organosilicas. Circular dichroism spectroscopy is commonly used for determination of the optical activity in the liquid state; however, solid-state CD spectroscopy can provide valuable information on chiral interactions or reactions, which occur specifically in the solid state.[33] Solid-state CD measurements have been reported on chiral organosilicas using KBr pellets.[34] In our case, measurements were carried out on the organosilicas dispersed in trichloromethane, which is an approximately isorefractive solvent, to avoid scattering contributions and depolarization effects at grain boundaries. However, evaluation of the data from solid-state CD measurements is still difficult, so the measurements should be considered as qualitative results. Circular dichroism measurements were carried out, first on the pure organosilicas dispersed in trichloromethane and then in combination with adsorbed benzoic acid. We assumed that if the chiral amine groups on the organosilica are accessible from the outside, interaction with the acidic chromophore should induce a significant optical activity of the otherwise achiral benzoic acid. Such induced circular dichroism is, for example, observed in solid-state inclusion compounds of achiral chromophores in chiral molecules.[35] For the here-described experiments, organosilica CBS-1 was used, which, although the silica with the smallest surface area, displays on the other hand the highest organic fraction of the described materials.

In Figure 6 the CD spectra of the pure organosilica (CBS-1) as well as measurements on a material previously contacted with benzoic acid are shown. The signal centered at ~206 nm for the pure organosilica (CBS-1) can be attributed to the amine groups attached to the chiral center. After addition of benzoic acid, two additional bands are observed in the CD spectrum due to the induced optical activity via adsorption of this chromophore on the chiral amines. The peaks centered at 247 and 274 nm can be attributed to adsorption peaks of benzoic acid of the respective UV spectrum.

Even though a qualitative evaluation of the chirality is hardly possible due to the fact that the sample is a solid, which makes the description of the concentration of the chiral centers difficult, this measurement clearly proves that the prepared organosilicas are indeed chiral: In addition, this chirality is accessible from the outside and influences molecules entering the pore system.

Conclusion

In conclusion, a new organosilica precursor for the generation of chiral and amine-functionalized organosilicas is presented. These precursors combine the three roles of a network builder, a chiral and latent functional group, and a porogen. The precursors are prepared by a convenient enantioselective hydroboration using (*S*)-monoisopinocampheylborane on an ethylene-bridged silica precursor. It could be shown that these precursors do self-organize after hydrolysis of their inorganic part via an aggregation of their organic parts into hydrophobic domains. Furthermore, it was shown that the size of the hydrophobic domains and therefore the resulting pore sizes could be tailored, depending on the chosen boron moieties. Quenching of the reaction with ethanol leads to a smaller template and corresponding small pores with average diameters of 2.0−2.6 nm, while the observed pore sizes are much larger (up to 5 nm) when a long-chain alcohol, e.g., hexadecanol, is added as a pendent side chain. After a condensation−ammonolysis sequence, amine-functionalized chiral mesoporous organosilicas are obtained. The highest surface areas were observed for organosilicas prepared with admixed pure inorganic precursors in a TEOS/CBS molar ratio of 4/1, yielding an organosilica with a surface area of 1010 m^2/g. However, it was also shown that the pure organosilica precursor is stable enough to at least partially maintain porosity, so that porous organosilicas with an organic monomer content of 100% could be prepared. All these direct organosilicas displayed disordered, wormlike pore systems.

It was shown that the presented monomers can also be used in a similar fashion as conventional PMO precursors: Common surfactants, such as the block copolymer F127, can be admixed to further control and tailor the resulting mesoporous system and finally create chiral *periodic* mesoporous organosilicas.

The chirality of the resulting organosilicas was proven using circular dichroism measurements. A strong optical activity was observed for the pure organosilica, attributable to the chiral amines in the framework. Addition of an achiral chromophore, benzoic acid, leads to an additional signal in

(33) Kuroda, R.; Honma, T. *Chirality* **2000**, *12*, 269.
(34) Yang, Y. G.; Suzuki, M.; Fukui, H.; Shirai, H.; Hanabusa, K. *Chem. Mater.* **2006**, *18*, 1324.
(35) Tanaka, K.; Kato, M.; Toda, F. *Chirality* **2001**, *13*, 347.

the CD spectrum indicative of the interaction of the benzoic acid with the chiral amines, proving that the chiral functional groups are indeed accessible for molecules entering the pores.

The described properties of the presented materials make them interesting for a variety of applications, especially in chromatography of optical isomers or enantioselective catalysis. Our current work is consequently devoted to the evaluation of the chiral discrimination potential of these materials. This approach should also be more versatile than only functionalization of amines: a great variety of other functional groups can be generated from borane compounds, as described in the literature. This could yield chiral organosilicas with tailor-made functionalities for many particular purposes. Furthermore, the self-organization motifs of these precursors can possibly be further advanced when the organic moieties on the boron groups are varied. Because all terminal alcohols or terminal alkenes can be attached to the remaining boron site, a variety of structure-directing motifs can be envisaged, possibly yielding interesting, predefined, and adjustable pore structures, functionalities, and morphologies of the resulting organosilicas.

Acknowledgment. The Max Planck Society is acknowledged for financial support through the ENERCHEM project. G.A.O. is the Government of Canada Research Chair in Materials Chemistry and Alexander von Humboldt Fellow (2005−2006). He is deeply indebted to the Natural Sciences and Engineering Research Council (NSERC) of Canada for sustained support of his PMO work. We thank Dr. Sebastian Polarz for helpful discussions.

Supporting Information Available: ^{1}H NMR spectra of reactants and products, FT-IR spectra, ^{13}C MAS spectra, nitrogen adsorption isotherm, NLDFT pore size distribution, and SAXS measurements (PDF). This material is available free of charge via the Internet at http://pubs.acs.org.

CM063026J